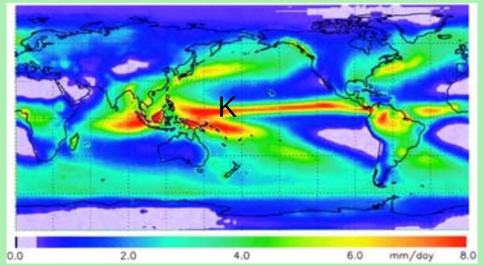

Joint Variability of Airborne Passive Microwave and Ground-based Radar Observations Obtained in the TRMM Kwajalein Experiment

Sandra E. Yuter[1], and David E. Kingsmill[2]

[1]North Carolina State University and [2]University of Colorado, CIRES and NOAA ESRL

Introduction

Goal: Use field experiment observations to evaluate the underlying physical theory of passive microwave precipitation retrieval that relates brightness temperatures (Tb) to surface rainfall (R_s).

- Satellite passive microwave precipitation retrievals, particularly over the tropical ocean, are key components of merged precipitation products such as the GPCP annual average map (above left).
- The detailed pattern of passive microwave precipitation rate (TMI) is often at odds with measurements from more accurate radar sensors (PR).

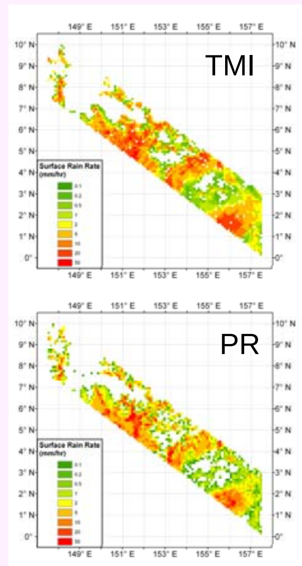

TRMM Microwave Imager (top) and Precipitation Radar (bottom) estimates of near surface rain rate in overpass southwest of Kwajalein on 4 July 2006. Data are remapped to 0.1 x 0.1 deg grid.

Data Sets and Methodology

The Tropical Rainfall Measuring Mission (TRMM) Kwajalein Experiment (KWAJEX) was held from July-September 1999 in the west Pacific and was designed to obtain an empirical physical characterization of precipitating convective clouds over the tropical ocean.

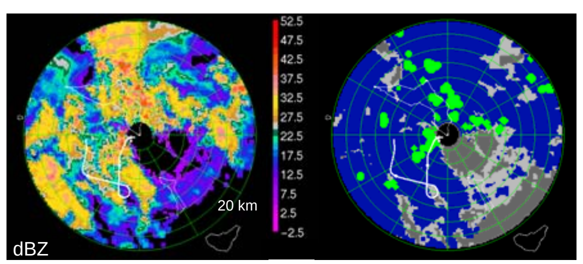

Example NASA DC-8 flight track on 3 September 1999. 20 min of DC-8 flight track is overlaid on low-level radar reflectivity (left) and a map (left) showing objectively classified convective (green) and stratiform (blue) regions. Light gray indicates Z < 15 dBZ and dark gray is no echo.

- Coordinated data sets were obtained from aircraft and ground-based sensors including passive microwave measurements from the Advanced Microwave Precipitation Radiometer (AMPR) on the NASA DC-8 aircraft and volumetric radar reflectivity data from a ground-based S-band radar (KPOL).
- AMPR and KPOL measurements were processed to yield over 24,000 temporal and spatial matching observations within 6 min coincidence.
  - The raining subset of 5 along-track x 4 cross-track AMPR pixels were averaged to yield 7 cross-track AMPR super-pixels (4 x 3.2 km^2)
  - Each AMPR super-pixel was matched to the nearest 2 x 2 km^2 interpolated KPOL radar pixel in 1.5 km altitude layers starting at 1.5 above sea level.

Table 1. Sample size of coincident AMPR and KPOL super-pixels categorized by subsets obtained within convective and stratiform regions and by incidence angle.

AMPR incidence angles	Convective Precipitation	Stratiform Precipitation
Angles 25.2° to -25.2°	7399	17370
Nadir only (0°)	1066	2553

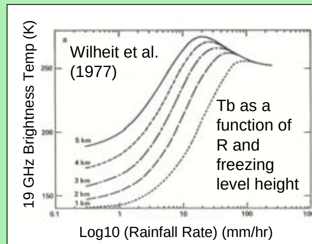

Passive microwave Tb are the result of column scattering and absorption properties of precipitation, cloud and water vapor. At frequencies < 22 GHz absorption by liquid water dominates. For a given freezing level height, absorption and associated Tb increase with increasing layer-average rain rate until about 20 mm/hr (42 dBZ). At frequencies > 60 GHz, ice scattering dominates and yields decreasing Tb for increasing ice particle concentration and size. Based on model output, the impact of partially melted particles on measured Tb is estimated to account for increases of up to 43 K at 10.7 GHz, 28 K at 19 GHz and 10 K at 85 GHz (Olson et al., 2001).

Several recognized sources of uncertainty in the relationship between passive microwave brightness temperatures and surface rainfall are minimized in the KWAJEX data sets:

- The freezing level height (rain layer depth) is nearly constant at 4787m±144m.
- Horizontal spatial resolution of the airborne radiometer data (19 GHz: 1.6 km, 85 GHz: 0.4 km) minimizes effects of inhomogeneous beam filling compared to TRMM satellite sensors (19 GHz: 35 km, 85 GHz: 7.7 km).
- AMPR nadir pixels observe the atmospheric column at 0° incidence angle compared to 53° incidence angle for TRMM TMI pixels.

⇒ Observed Tb and R_s should be better correlated in KWAJEX data sets than in TRMM satellite data for this geographic region.

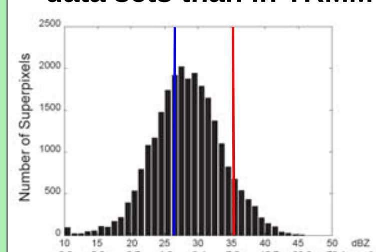

Cartesian-interpolated KPOL rain layer reflectivity (1.5 – 3 km altitude, 2 km horizontal resolution) is used as a proxy for surface rain rate (R_s)

$$dBZ/10 \sim \log_{10}(a) + b \times \log_{10}(R)$$

a=160 and b=1.5 based on Kwajalein disdrometer data (Houze et al., 2005)

Distribution of super-pixel rain-layer reflectivities and associated rain rates, vertical lines are modes of the overlapping distributions for stratiform (blue) and convective (red) precipitation subsets.

Synergistic Findings from Related Studies

Typical Kwajalein MCSs contain few convective lines and often have embedded convective cells interspersed within stratiform regions (Holder et al., 2008).

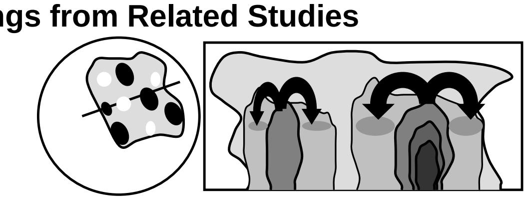

Schematic horizontal and vertical views of typical Kwajalein MCS. Darker shading represents higher reflectivity. Arrows show idealized particle trajectories.

Microphysics probe data from the NASA DC-8 and UND Citation (Sukovich et al. 2008) indicates that ensembles dominated by aggregates occur in both convective and stratiform precipitation regions. Graupel preferentially occurred in convective regions and at temperatures > -10°C. The mean volume diameter of ensembles of ice particles is skewed toward smaller sizes. D < 2 mm for most graupel particles.

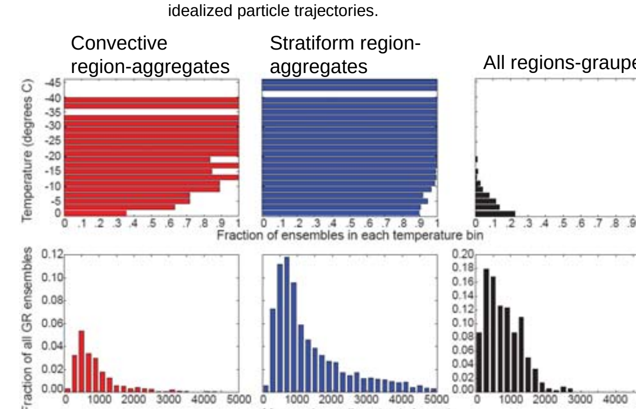

Results

- Variability in R for a given Tb is larger for convective compared to stratiform regions.
- The modes in the distribution of Tb for convective and stratiform subsets are most distinct at 19 GHz (74 K difference) compared to ≤ 10 K difference for 85 and 10.7 GHz.
- At 3.4 mm/hr (30 dBZ), Tb varies >75K at 19 and 10.7 GHz and >100 K at 85 GHz

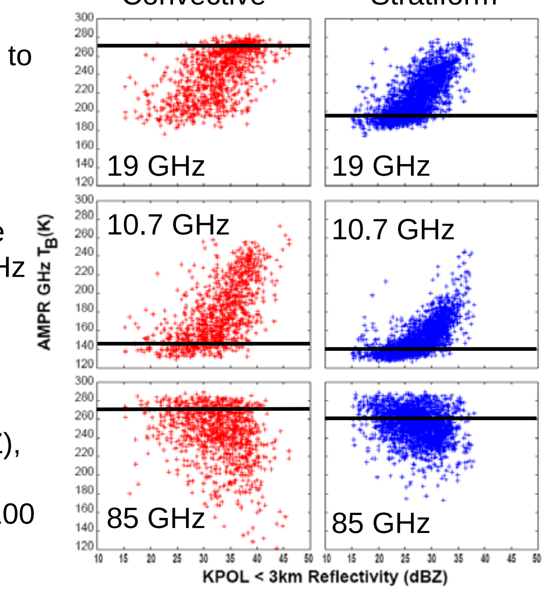

Scatterplots of super-pixel KPOL rain layer reflectivity and AMPR nadir-only Tb for indicated channels. (left column) convective precipitation regions, (right column) stratiform precipitation regions. Horizontal lines indicate mode in distribution of all AMPR super-pixels in that category. Distributions for all AMPR points (not shown) are similar to nadir points.

Conclusions

- For tropical, open ocean, deep convection observed in KWAJEX, there is a factor of 4 variation in R for a given Tb when relating aircraft-observed Tb to rain-layer rain rate.
  - Observed variation in 19 GHz Tb for a given R is equivalent to ~4 km variability in freezing level height in Wilheit et al. (1977) calculations.
- Uncertainties in relating Tb to R are larger in convective precipitation regions compared to stratiform regions which have narrower melting layers and more large ice particles (D > 2 mm).
  - Model-based estimates of the impact of partially melted particles account for less than half of the observed Tb variation.
- The current use of TMI 85 GHz Tb for the detailed rain rate pattern in TRMM products is likely a large source of error in these patterns since higher spatial resolution 85 GHz Tb at 0° incidence contain little information on the rain-layer rain rates.
- The practical impact of the poor instantaneous correlations between Tb and R and resulting uncertainties in rainfall retrieval will be difficult to mitigate unless satellite sensors can distinguish among precipitation structures that yield different sub-ranges of Tb for a given R.
- Satellite passive microwave may be better suited to area-threshold methods of precipitation estimation (e.g. GPI) rather than quantitative rain rate retrieval.

Acknowledgements: Thanks to Song Yang, Frank LaFontaine, Ellen Sukovich, Matt Miller, and David Spencer. This work was supported by NASA PMM grants NNG04GJ15G and NNG04GA65.